Numerical Estimation of Angle of Incidence with Bleistein Approach

Ritesh K. Sharma,Gary F. Margrave

ABSTRACT

The angle of incidence, θ_i, of a ray is the angle measured from the ray to the reflector normal. Historically, ray tracing is used to compute the angle of incidence. According to ray tracing, a wave can be modeled as a large number of rays (narrow beam), and a ray can be considered locally straight over a very small distance. In ray tracing, Snell's law is used to compute ray path and the angle of incidence. We investigate a method to compute the angle of incidence from the ratio of two reflectivity attributes known as β (reflectivity function) and β_1. Another method, the ratio of β_2 and β_1, is also proposed to compute the angle of incidence with less computation. The basic objective of this paper is to verify the proposed approach numerically. A comparative study of the two methods, β/β_1 and β_2/β_1, is considered here.

INTRODUCTION

According to ray theory, when a ray from the source hits a reflective surface, it generates both reflected and transmitted rays and the angles of reflection and transmission are governed by Snell's law. In ray tracing, the ray parameter is conserved for a ray along its path in a medium (Shearer, 1999). The ray parameter, p, is related to the angle of incidence,θ by $p = \sin\theta/c$, where c is the velocity of the medium. Traditionally, the ray parameter is computed from the recorded data (Margrave, 2002). Once the ray parameter is known, the angle of incidence can be computed using above relation. Alternatively Bleistein, Cohen and Stockwell's (Bleistein et al., 2000) approach can be used to compute the angle of incidence. Here, the background theory of perturbation theory is discussed and we describe how they propose to compute the angle of incidence.

In the forward problem, the material parameters, boundary conditions and source mechanism are known to derive the wavefield by solving the equation or set of equations which relate the wavefield to the input parameters. In the inverse problem, the scattered field is known at the surface and the unknowns are the material parameters and their discontinuity surfaces, known as reflectors. The ultimate goal of the forward scattering problem is to derive an integral equation from which the wavefield can be described at a specific receiver location due to a source located at a different position (Bleistein et al., 2000). This equation is then converted to a solution of the inverse problem. Green's theorem and Helmholtz equation (Green's functions) are essential tools for the forward scattering problem. There is always a problem associated with Green's function because the exact Green's function is seldom known. Thus approximations of the Green's function are often used in the calculation. In forward modeling, an approximate wave speed profile is used whether or not the exact Green's function is known. Perturbation theory is then used to relate the approximate wavespeed profile and Green's function to their true counterparts. According to this theory, the true wavefield is the sum of the incident wavefield and the scattered field. Since incident wavefield and wavespeed are known, modeling formula will represent the scattered wave-

field in terms of the perturbation in wavespeed. Using this theory, an integral equation for the scattered wavefield at the receiver location is known in terms of known incident wavefield, unknown scattered wavefield and unknown perturbation. Thus, the resulting equation is non linear and is linearized using the Born-approximation. In the inverse problem, the objective is to determine the perturbation from the observed data at the surface. Further, to get the band limited version of perturbation, the objective is redefined and is referred to as the reflectivity function β. A similar inversion attribute, β_1, can also be obtained using the same approach. These two attributes differ by a factor of $2\cos\theta/c$, where θ is the opening angle and c is the velocity. There are known expressions for peak values of β and β_1. These two operators, β_{peak} and β_{1peak} differ by a factor of $2\cos\theta_s/c$ which allow us to estimate the angle of incidence θ_s, without knowing the different specular source-receiver pair that produces the distinct value of incident angles. Another inversion attribute, β_2 is also proposed which can be constructed similarly to β_1. The ratio of β_2 and β_1 is used to estimate the angle of incidence and this takes fewer computation than the ratio of β and β_1. In this report we verify the above statements numerically.

METHODOLOGY

In the forward scattering problem the total wavefield, $\Psi(x, x_s, \omega)$ is the monochromatic wavefield at x due to a source located at x_s, and satisfies the Helmholtz equation

$$\left(\nabla^2 + \frac{\omega^2}{v^2}\right)\Psi = -F(\omega)\,\delta(x - x_s), \tag{1}$$

where $F(\omega)$ is the spectrum of the source and $\delta(x - x_s)$ is the spatial impulse. Here $x = (x_1, x_2, x_3)$ and $x_s = (x_{1s}, x_{2s}, x_{3s})$. v is the velocity as a function of position. Presently, according to perturbation theory, $v(x)$ is unknown and related to known back ground velocity as

$$\frac{1}{v^2} = \frac{1}{c^2}(1 + \alpha(x)) \tag{2}$$

where $\alpha(x)$ is the perturbation. As per scattering theory, the total field is described as the sum of the incident wavefield and the scattered wavefield according to equation (3)

$$\Psi = \Psi_I + \Psi_S \tag{3}$$

where Ψ_I is the incident wavefield and satisfies the Helmholtz wave equation whereas Ψ_S is the scattered wavefield and satisfies the perturbed Helmholtz equation. By employing both Green's theorem and the Helmholtz equation for the incident and scattered wavefields, the integral equation for the scattered wavefield at the receiver location, x_g, due to a source located at x_s can be written as

$$\Psi_s(x_g, x_s, \omega) = \omega^2 \int \frac{\alpha}{c^2}[\Psi_I(x, x_s, \omega) + \Psi_S(x, x_s, \omega)]\, g(x_g, x, \omega)\, d^3x \tag{4}$$

where $g(x, x_g, \omega)$ is the Green's function. This equation shows that the scattered field is a function of unknown perturbation $\alpha(x)$ and the scattered field itself. Thus, this equation is non linear. Using the Born approximation, the scattered wavefield is assumed to be much less than incident wavefield. Following the Born-approximation, the product of the

scattered wavefield and perturbation is removed from the right side of equation (4) and thus, the modeling formula can be described as the linearized version of equation (4)

$$\Psi_s\left(x_g, x_s, \omega\right) = \omega^2 \int \frac{\alpha}{c^2} \Psi_I\left(x, x_s, \omega\right) g\left(x_g, x, \omega\right) d^3x. \tag{5}$$

Now, the main objective of the inverse problem is to determine the perturbation α from the observed data. This is obtained by taking the inverse of the equation (5) (Bleistein et al., 2000) and expressed as

$$\alpha\left(y\right) = \frac{1}{8\pi^3} \int d^2\xi \frac{\left|h\left(y,\xi\right)\right|}{a\left(y,\xi\right)\left|\nabla_y \phi\left(y,\xi\right)\right|} \int d\omega e^{-i\omega\phi(y,\xi)} \Psi_s\left(x_s, x_g, \omega\right) \tag{6}$$

where $\left|h\left(y,\xi\right)\right|$ is Beylkin determinant, $a\left(y,\xi\right)$ is the amplitude spreading factor and ξ defines the co-ordinates of the acquisition surface. Term $\phi\left(y,\xi\right)$ contains the travel time information.

Due to the band limited nature of real-world experimental data, a band limited version of α is required. Further, by taking the gradient of the band limited version of α, a new function, namely the reflectivity function can be obtained. Thus, to correct for band limiting, our goal is redefined as to obtain the reflectivity function from the observed data. The reflectivity function β can be obtained from equation (6) by taking the derivative of α and is

$$\beta\left(y\right) = \frac{1}{8\pi^3} \int d^2\xi \frac{\left|h\left(y,\xi\right)\right|}{a\left(y,\xi\right)\left|\nabla_y \phi\left(y,\xi\right)\right|} \int i\omega d\omega e^{-i\omega\phi(y,\xi)} \Psi_s\left(x_s, x_g, \omega\right). \tag{7}$$

2.5D Inversion

Traditionally, seismic data is collected along a straight line whenever possible. This type of collected data is two dimensional $(2D)$. It is known that an inversion formula using 2D assumption will not recover amplitude correctly (Bleistein et al., 2000). However, it can be recovered using the inversion formulas which are obtained from the 3D expressions by applying the methods of high frequency asymptotic to 3D expressions. This type of formulation is called 2.5D formulation and it recovers the amplitude variation correctly for 2D data.

Common-Shot Inversion

Common-shot geometry can be described by a fixed source location and spatially varying receiver positions. After putting the values of Beylkin determinant, amplitude factor and phase term for 2D in the expression of the reflectivity function, equation (7), the reflectivity function can be simplified further and expressed as

$$\beta\left(y\right) = \frac{4y_3}{\sqrt{2\pi c^3}} \int d\xi \frac{\sqrt{r_s + r_g}}{r_g^{(3/2)}} \sqrt{r_s} \cos\theta \int \sqrt{\omega} d\omega e^{-i\omega\phi(y,\xi) + i\pi/4 sgn(\omega)} \Psi_s\left(x_g, x_s, \omega\right) \tag{8}$$

where r_s is the distance between shot point and scattering point and r_g is the distance between the receiver point and scattering point. Another reflectivity estimate, β_1, can be

obtained by multiplying $|\nabla_y \phi|$ in the denominator of the equation (7). This inversion attribute is expressed as

$$\beta_1(y) = \frac{2y_3}{\sqrt{2\pi c}} \int d\xi \frac{\sqrt{r_s + r_g}}{r_g^{(3/2)}} \sqrt{r_s} \cos\theta \int \sqrt{\omega} d\omega e^{-i\omega\phi(y,\xi) + i\pi/4 sgn(\omega)} \Psi_s(x_g, x_s, \omega). \quad (9)$$

Finally, another reflectivity function, β_2, can be obtained by removing the $|\nabla_y \phi|$ from the denominator of the equation (7) and expressed as

$$\beta_2(y) = \frac{8y_3}{\sqrt{2\pi c^5}} \int d\xi \frac{\sqrt{r_s + r_g}}{r_g^{(3/2)}} \sqrt{r_s} \cos\theta \int \sqrt{\omega} d\omega e^{-i\omega\phi(y,\xi) + i\pi/4 sgn(\omega)} \Psi_s(x_g, x_s, \omega). \quad (10)$$

The peak values of the above inversion estimates are also known (Bleistein et al., 2000) and given by

$$\frac{\beta_{peak}}{\beta_{1peak}} \sim \frac{2\cos\theta_s}{c} \quad (11)$$

and

$$\frac{\beta_{2peak}}{\beta_{1peak}} \sim \frac{4\cos^2\theta_s}{c^2} \quad (12)$$

where θ_s is the angle of incidence. Equations (11) and (12) allow us to compute the cosine of the angle of incidence with out ever having to determine the specular source -receiver pair. It is proposed that time taken for estimating the angle of incidence by equation (12) is less than by equation (11). The verification of above statements is shown numerically in the next section.

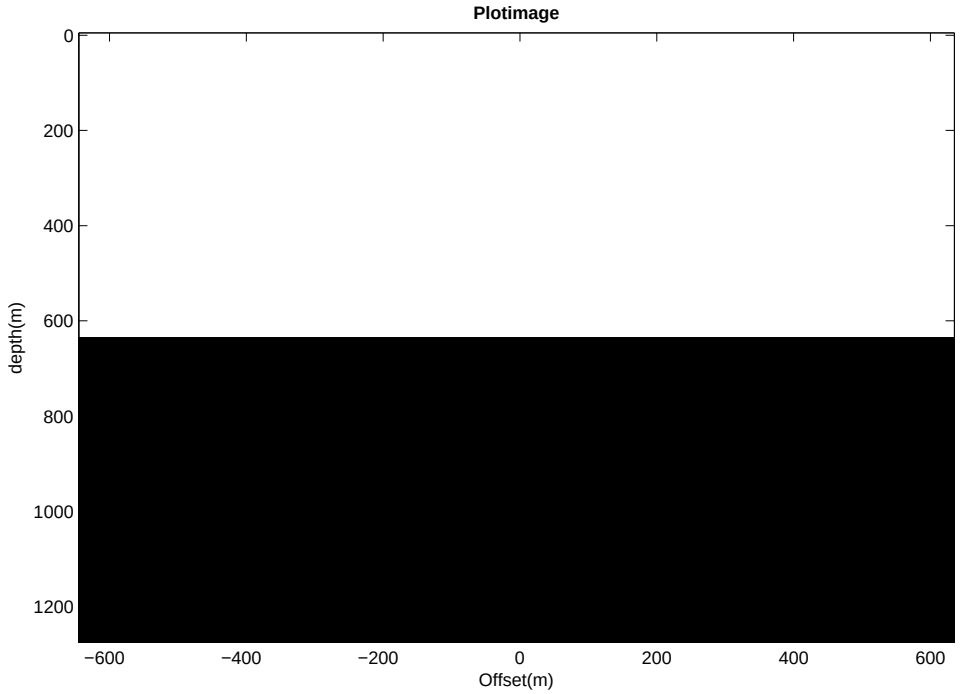

FIG. 1. model

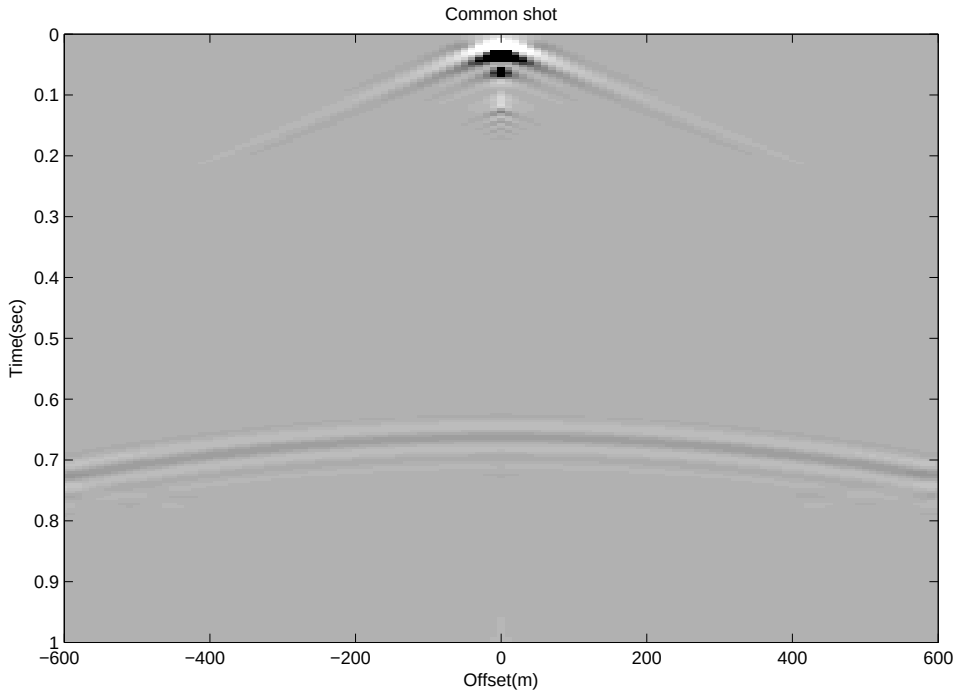

FIG. 2. Common-shot seismic section across the model.

NUMERICAL EXAMPLE-A DISCUSSION OF RESULTS

Model 1

Model parameters are given in the appendix. Figure (1) shows a model in which a single reflector is defined. Figure (2) shows the common-shot seismic section, created with MATLAB function, $afd\_\ shotrec\_alt$, of the CREWES MATLAB tool box. The source is taken at the center of the model with receivers on the surface in the split-spread pattern. The inversion for the reflectivity function is shown in figure (3). In addition to obtaining the reflectivity function, a MATLAB function is written on the basis of the equation (8). Further, two more MATLAB function are written on the basis of the equations (9) and (10) to obtain β_1 and β_2, respectively. These two functions are shown in figures (4) and (5). It is demonstrated from figures (3), (4) and (5) that degradation of resolution can be seen away from the center of the model. Figure (6) shows the value of the cosine of the incident angle with offset. Presently, the angle of incidence is computed from the ratio of β/β_1 , β_2/β_1, and using simple trigonometry. This figure demonstrates that the values of the cosine of the incident angle, extracted from β/β_1 , β_2/β_1 are approximately same but differ from the expected values, computed by using simple Pythagorean theorem. Extracted and expected values are the same at the center of the model. Here, a falloff in accuracy with the falloff in resolution with increasing offset is seen. The extracted values are differing from the expected values with offset because of lack of focused energy with offset, as mentioned before. By using relation, percentage error $=$ (|Extracted value- Expected value|/Expected value), the percentage error in the estimation of the cosine of incident angle is shown in figure (7). This demonstrate that error is zero or near to zero at the center of model but increasing with offset. Further, the maximum percentage error with far offset is 6.5% approximately which is acceptable.

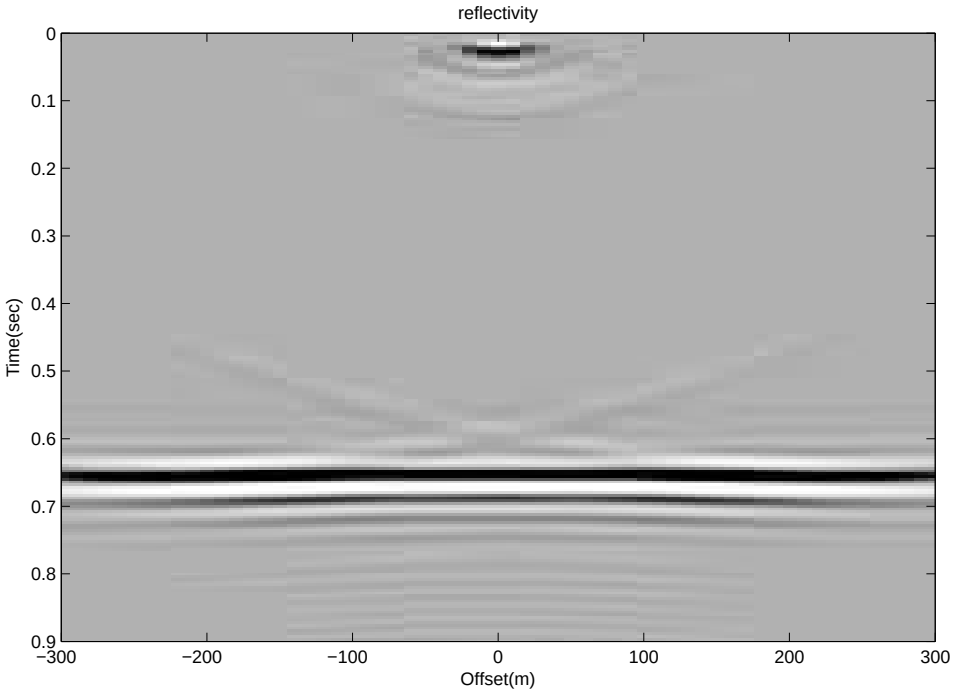

FIG. 3. Inversion for the reflectivity function(β).

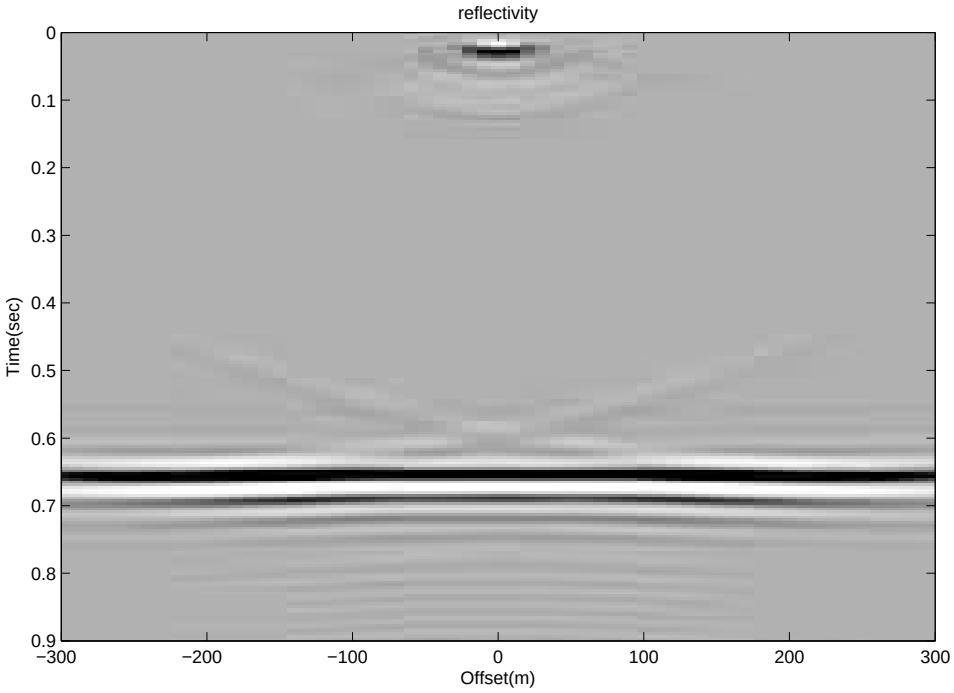

FIG. 4. Reflectivity function multiplied times the cosine of the incident angle(β_1.)

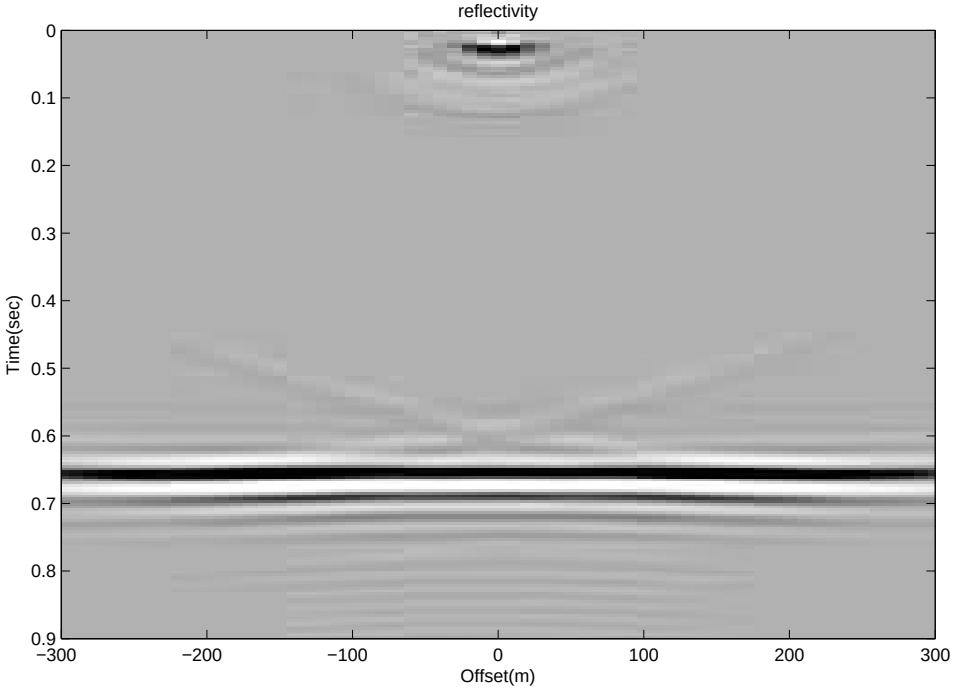

FIG. 5. Inversion for the reflectivity function multiplied times the cosine square of the angle(β_2).

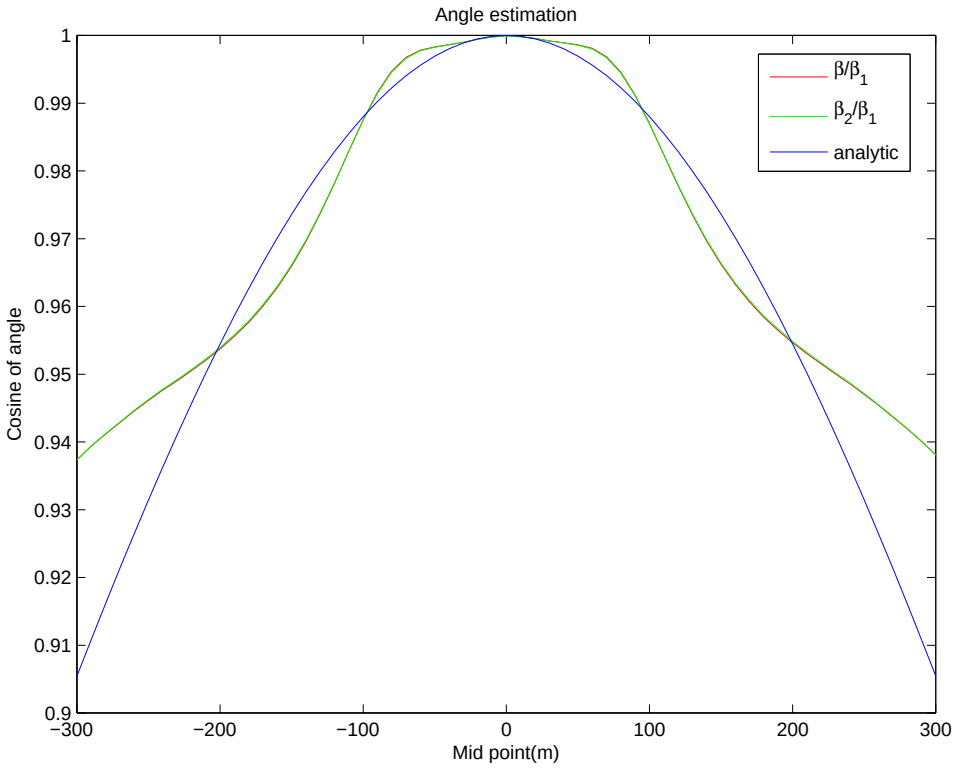

FIG. 6. Estimation of angle of incidence with proposed methods and compared with analytic one.

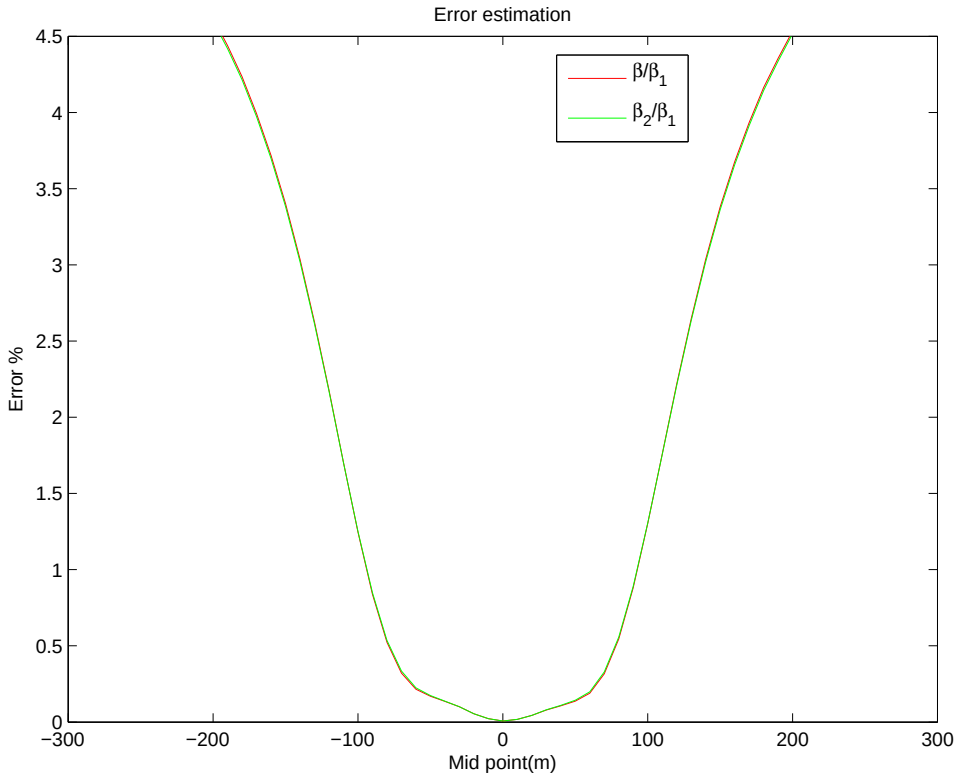

FIG. 7. Percentage error in computing angle of incidence from proposed methods.

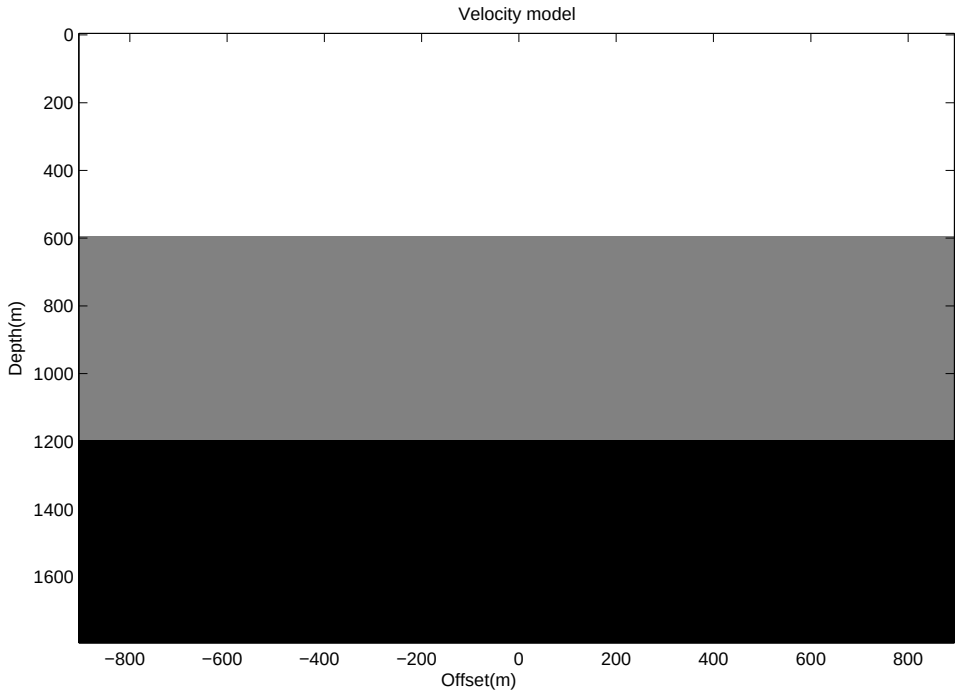

FIG. 8. Velocity model for two layer.

Model 2

Model parameters are given in the appendix. Figure (8) shows a model in which two reflectors are defined. The common-shot seismic section, created with MATLAB function $afd\_\ shotrec\_alt$ of the CREWES MATLAB tool box, is shown in figure (9). This figure is plotted with a higher clipped display than the display of figure (2), otherwise, only first hyperbolic reflection, the response of first layer, would be visible with less resolution. Thus, the focused energy is less here in comparison of model 1. Further, the degradation of resolution of the second reflector's image at zero offset compared to the resolution of the first reflector is seen here. The inversion for the reflectivity function is shown in figure (10). The reflectivity functions, β_1 , β_2 are shown in figures (11) and (12). The loss of the resolution of the reflectors image is demonstrated from the figures (10), (11) and (12). Figure (13) shows the values of the cosine of the incident angle for first layer, extracted from the ratios of the β/β_1, β_2/β_1 and computed by using simple Pythagorean theorem. Again, values are matching at the center of the model and varying with offset. As seen from the figures (10), (11), (12), the lacking of focused energy is seen here, thus, the extracted values differ from the expected values at the central part of the model more in model 2 than in model 1. Figure (14) shows the values of the cosine of incident angle for second layer computed with a MATLAB function of ray tracing, $traceray\_pp$ and due to lack of focused energy extracted values are differing from the computed. The error in the estimation of the cosine of the incident angle for second layer is shown in figure (15). This demonstrates that error is not zero as expected at the central part of the model but it is near to zero. The maximum percentage error with offset is about 4.5%. A ray tracing for second layer is shown in figure (16) which is created with a MATLAB function, $traceray\_pp$ and is used to compute the angle of incidence. The MATLAB function,$traceray\_pp$, gives the ray parameter and the angle of incidence is computed by relation,$p = \sin\theta/v$, because velocity is known, here. Now, the times taken by the ratios, β/β_1 and β_2/β_1 are computed. Figure (17) shows the comparison of times which are taken by methods 1 and 2 for different 2D model. Presently, β/β_1 and β_2/β_1 are taken as method 1 and 2. This figure shows that time taken by both of these methods are approximately same for both 2D models respectively. Both methods are applied also on joanna_channel(Margrave and Cooper, 2007). Subplot of figure (17) shows that in the case of joanna_channel, time taken by method 2 is less than the time of method 1.

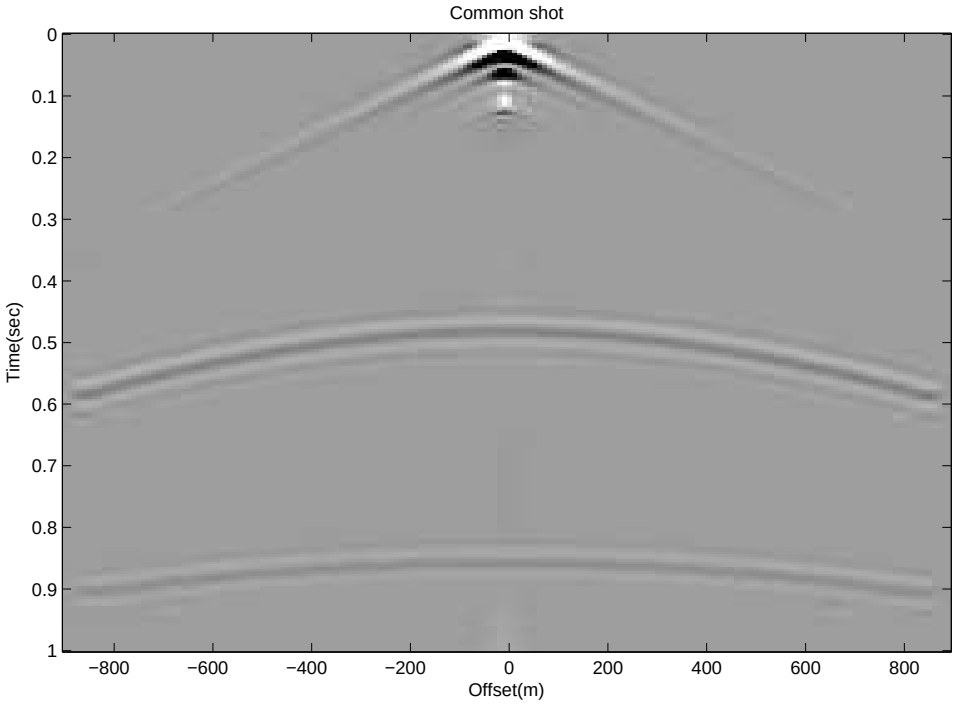

FIG. 9. Common-shot seismic section.

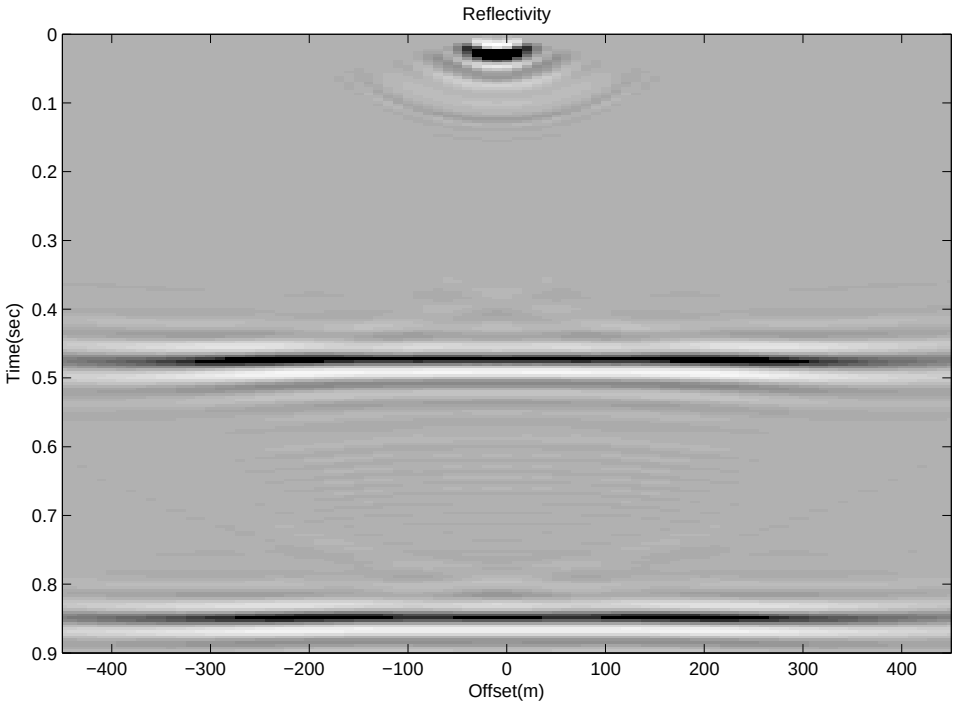

FIG. 10. Inversion for the reflectivity(β).

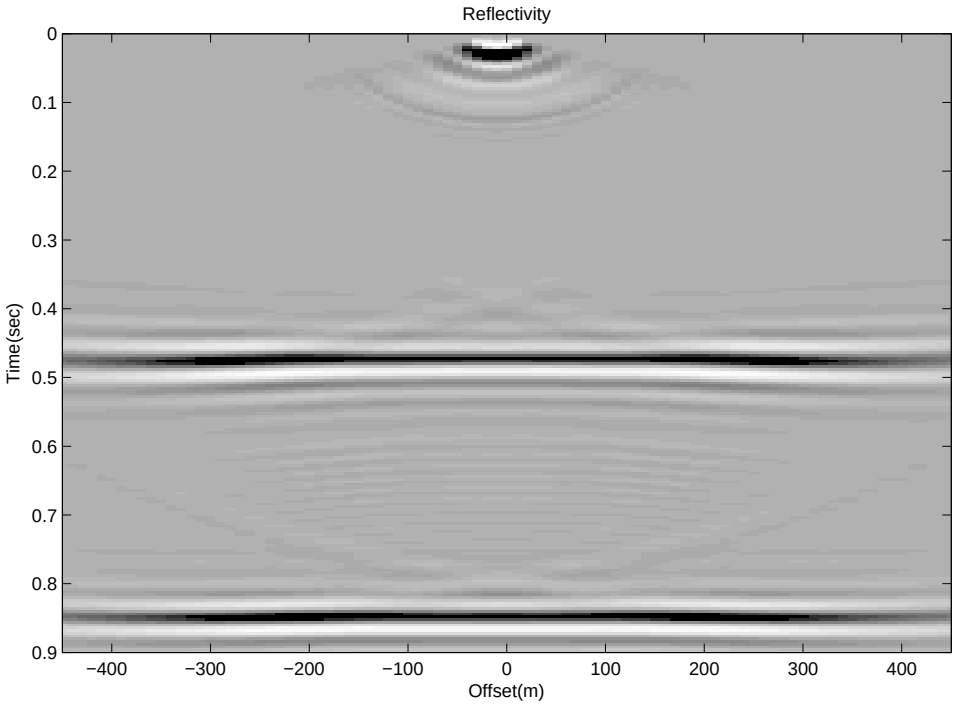

FIG. 11. Inversion for the reflectivity multiplied by the cosine of the angle(β_1).

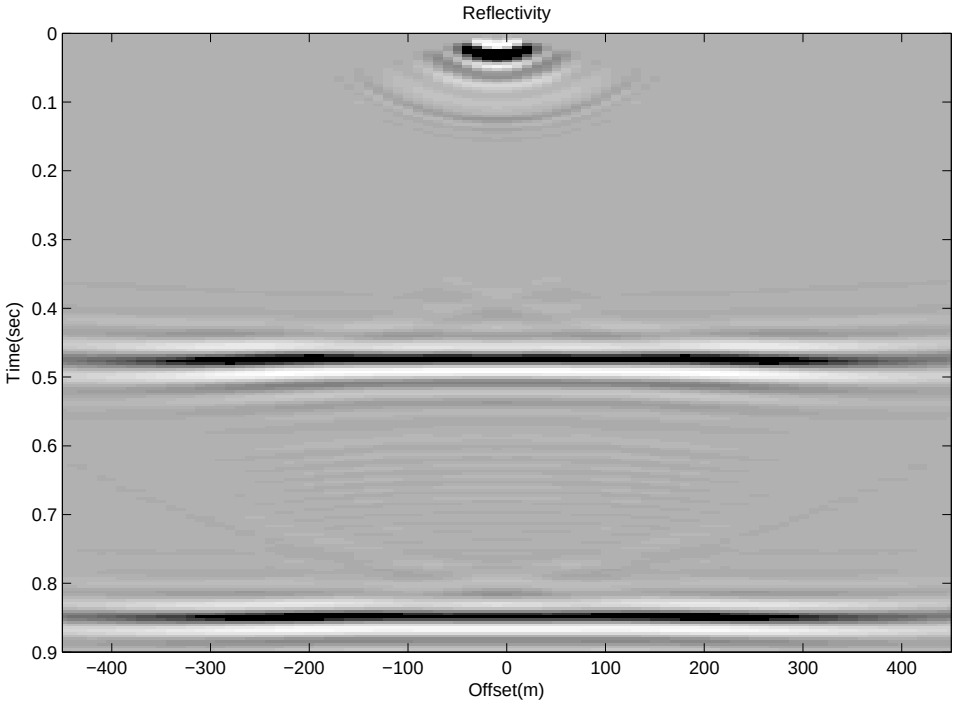

FIG. 12. Inversion for the reflectivity multiplied by the cosine square of the angle(β_2).

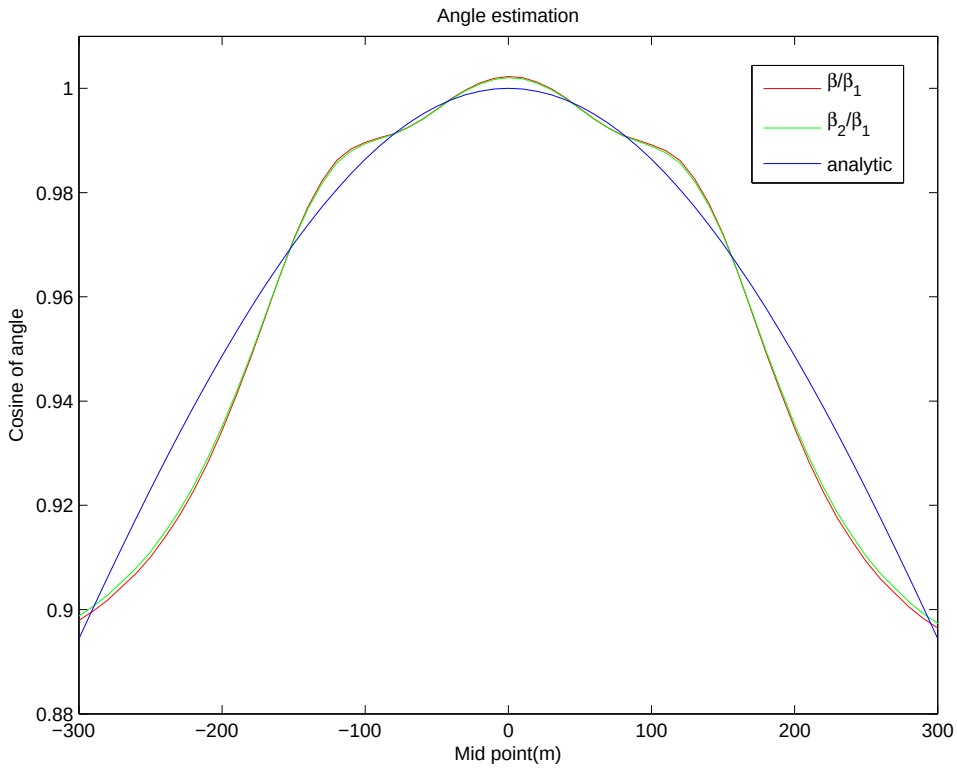

FIG. 13. Values of the cosine of the incident angle for 1st layer.

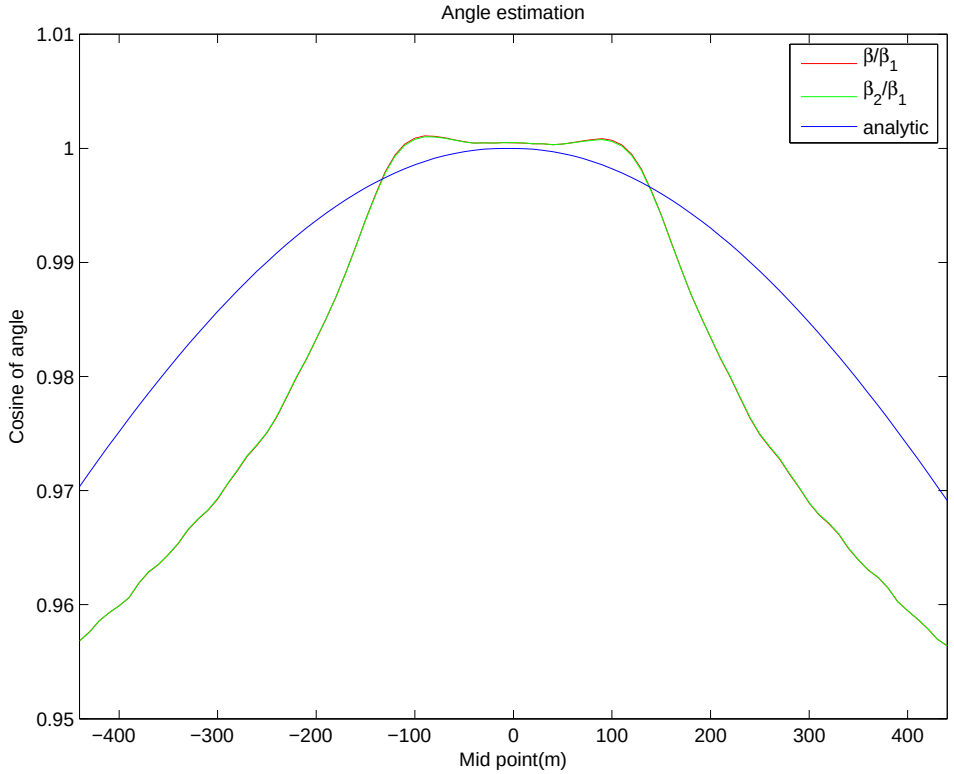

FIG. 14. Estimation of the cosine of the incident angle for 2nd layer.

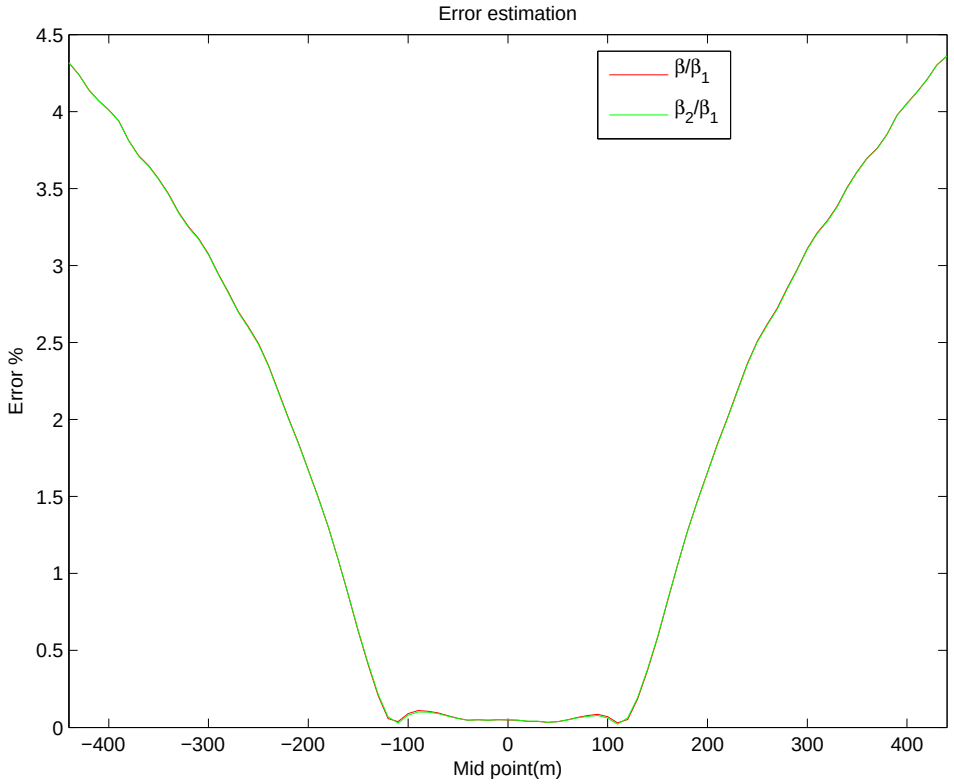

FIG. 15. Error estimation for 2nd layer.

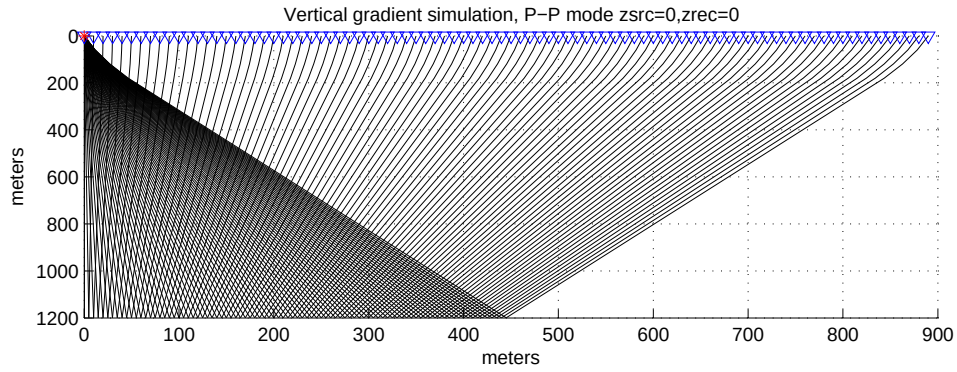

FIG. 16. Ray tracing for second layer.

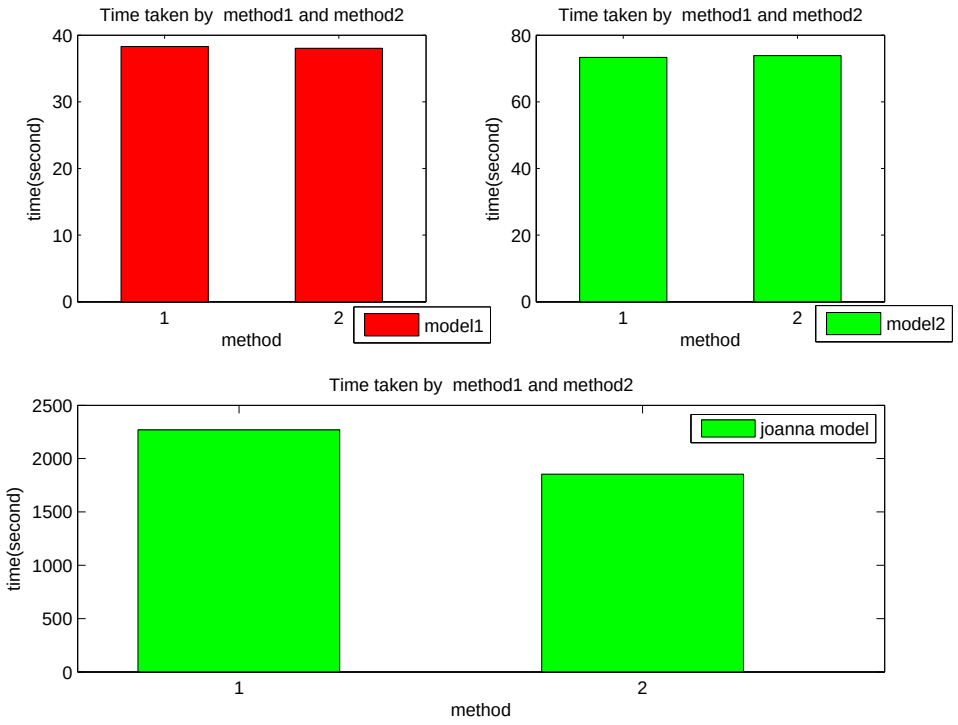

FIG. 17. Time comparison of proposed methods for different models.

CONCLUSION

The specular angle of incidence can be computed with both methods, namely, the ratio of β/β_1 and the ratio of β_2/β_1. Both of these methods give approximately the same result for both the models. At the central part of the model the extracted values of the angle of incidence match with the computed values. The results may be improved with a common-shot seismic section of high resolution. Computationally, the time taken by both of these methods is same for 2D models but for 3D model, method 2 is more efficient than 1. Method 2 takes 18% lesser time than time of method 1.

REFERENCES

Bleistein, N., Cohen, J. K., and Stockwell, J. W., 2000, Mathematics of Multidimensional Seismic Imaging,Migration,and Inversion: Springer.

Margrave, G. F., 2002, Methods of Seismic Data Processing: Course Notes.

Margrave, G. F., and Cooper, J. K., 2007, Seismic modeling in 3d for migration testing: CREWES Research Report, **19**, 5–10.

Shearer, P. M., 1999, Introduction to Seismology: Elesvier.

APPENDIX

Depth(meter)	Velocity(meter/sec.)
0	2000
630	2000
640	3000
1270	3000

Table 1. The depth and velocity of model 1

Depth(meter)	Velocity(meter/sec.)
0	2600
590	2600
600	3200
1190	3200
1200	3800
1790	3800

Table 2. The depth and velocity of model 2